Short Article

Developmental Cell

Iroquois Proteins Promote Skeletal Joint Formation by Maintaining Chondrocytes in an Immature State

Graphical Abstract

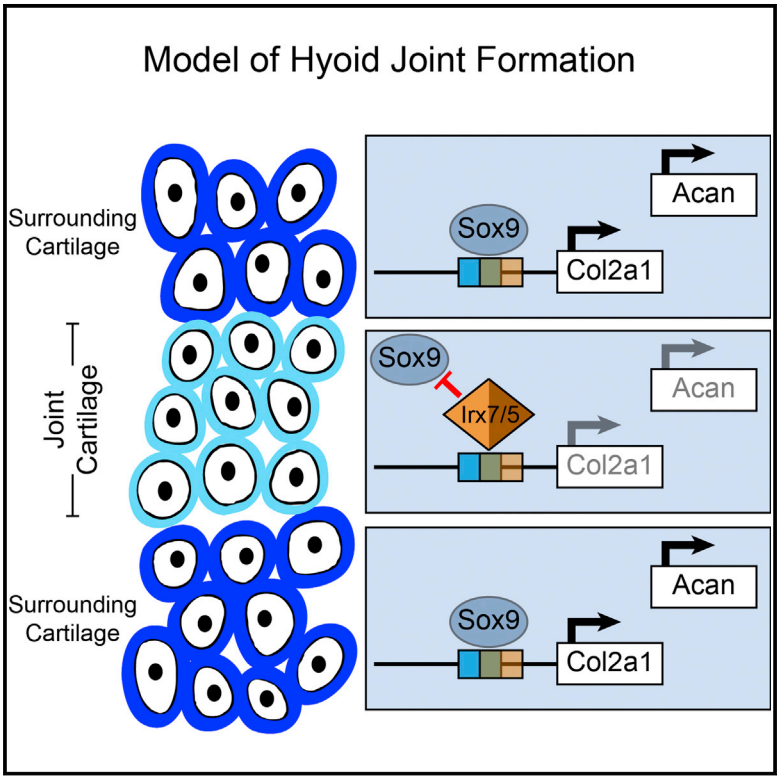

Highlights

- Iroquois proteins are required for skeletal joint development
- Irx7 and Irx5a inhibit chondrocyte maturation at the zebrafish hyoid joint
- Irx7 binding prevents Sox9 activation of a cartilage type II collagen enhancer
- Mouse IRX1 can also inhibit maturation of mammalian cartilage cells

Authors

Amjad Askary, Lindsey Mork, Sandeep Paul, ..., Rodney Dale, Francesca V. Mariani, J. Gage Crump

Correspondence

gcrump@usc.edu

In Brief

Askary et al. elucidate roles for Iroquois transcriptional repressors in the development of the zebrafish hyoid joint. They show that Iroquois proteins maintain cartilage cells in an immature state, an essential feature of both fish and mammalian joints, in part by preventing activation of matrix genes by Sox9.

Askary et al., 2015, Developmental Cell *35*, 358–365
November 9, 2015 ©2015 Elsevier Inc.
http://dx.doi.org/10.1016/j.devcel.2015.10.004

CellPress

Developmental Cell
Short Article

Iroquois Proteins Promote Skeletal Joint Formation by Maintaining Chondrocytes in an Immature State

Amjad Askary,[1] Lindsey Mork,[1] Sandeep Paul,[1] Xinjun He,[1] Audrey K. Izuhara,[1] Suhasni Gopalakrishnan,[1] Justin K. Ichida,[1] Andrew P. McMahon,[1] Sonja Dabizljevic,[2] Rodney Dale,[2] Francesca V. Mariani,[1] and J. Gage Crump[1,*]
[1]Eli and Edythe Broad Center for Regenerative Medicine and Stem Cell Research, University of Southern California, Los Angeles, CA 90033, USA
[2]Department of Biology, Loyola University Chicago, Chicago, IL 60660, USA
*Correspondence: gcrump@usc.edu
http://dx.doi.org/10.1016/j.devcel.2015.10.004

SUMMARY

An early event in skeletal joint development is the specification of articular chondrocytes at the joint surface. Articular chondrocytes are distinct in producing lower levels of cartilage matrix and not being replaced by bone, yet how they acquire these properties remains poorly understood. Here, we show that two members of the Iroquois transcriptional repressor family, Irx7 and Irx5a, function to block chondrocyte maturation at the developing hyoid joint of zebrafish. These Irx factors suppress the production of cartilage matrix at the joint in part by preventing the activation of a *col2a1a* enhancer by Sox9a. Further, both zebrafish Irx7 and mouse IRX1 are able to repress cartilage matrix production in a murine chondrogenic cell line. Iroquois proteins may therefore have a conserved role in keeping chondrocytes in an immature state, with the lower levels of cartilage matrix produced by these immature cells contributing to joint flexibility.

INTRODUCTION

Joints provide essential mobility to the vertebrate skeleton, with degeneration of joints in arthritis a leading cause of disability in humans (Hootman et al., 2012). Most joints follow a common developmental sequence. From an early pre-cartilage condensation, a subset of cells within the ''interzone'' are specified as articular chondrocytes while flanking cells mature into hypertrophic chondrocytes (Hartmann and Tabin, 2001; Archer et al., 2003). Unlike growth plate chondrocytes, articular chondrocytes are not replaced by bone and rapidly shut off *Col2a1* expression, which may aid in this tissue serving as a flexible cushion for joint surfaces. The larval zebrafish face has at least two sets of bilateral joints that appear to replicate the first stage of interzone formation: a ''jaw joint,'' which articulates Meckel's and palatoquadrate cartilages, and a ''hyoid joint,'' connecting hyomandibular and ceratohyal cartilages via a small interhyal cartilage (Figures 1A and 1B).

A number of studies point to a critical balance between Gdf/Tgfβ and Bmp signaling in specifying articular versus hypertrophic chondrocyte fates at the interzone, yet their downstream targets are not well understood (Francis-West et al., 1999). *Gdf5* and *Gdf6* are expressed within the joint interzone and required for joint formation within the mouse limb (Settle et al., 2003). Conversely, the expression of Bmp antagonists, such as *Chordin* and *Noggin*, within the interzone suggests an important role of Bmp repression in promoting joint development (Brunet et al., 1998; Hartmann and Tabin, 2001; Nichols et al., 2013). In support of this, Tgfβ and Bmps can bias the adoption of articular versus hypertrophic fates, respectively, upon chondrogenic differentiation of murine embryonic stem cells (Craft et al., 2013). Here, we show that transcriptional repression by Bmp signaling localizes expression of *irx7* and *irx5a* to the developing hyoid joints.

Iroquois proteins are thought to function largely as transcriptional repressors (Cavodeassi et al., 2001). While there are three members of the Iroquois family in *Drosophila* (Gomez-Skarmeta et al., 1996; McNeill et al., 1997), most terrestrial vertebrates have six members arranged into two genomic clusters: *Irx1/2/4* and *Irx3/5/6*. These Irx genes are expressed within the developing avian and murine limbs, with the *Irx1/2/4* cluster expressed in interzone regions of the digit joints and *Irx3/5/6* in mesenchyme flanking each digit (McDonald et al., 2010). A role of Irx genes in limiting skeletal development is suggested by fusions of the distal phalanges in the spontaneous *Fused toes* mouse, which contains a large heterozygous deletion encompassing the *Irx3/5/6* cluster and three other genes (Grotewold and Rüther, 2002; Peters et al., 2002). Interestingly, an additional non-clustered Irx gene—*irx7*—exists in only fishes, and we find it to be expressed uniquely at the developing hyoid joint. Here, we show that Irx7, together with Irx5a, cell autonomously repress high-level expression of cartilage matrix genes within the less mature chondrocytes of the joint interzone.

RESULTS AND DISCUSSION

Expression of *irx7* and *irx5a* within the Developing Hyoid Joint

In an expression screen of the developing zebrafish face, we detected early and persistent expression of *irx7* and *irx5a* within the joint-forming region of the second pharyngeal arch. At 36-hr post-fertilization (hpf), prior to cartilage differentiation, we observed restricted expression of *irx7* within *dlx2a*+ mesenchymal cells of the intermediate hyoid arch, with additional weak expression in the first pharyngeal pouch (Figure 1C). Previous lineage tracing had shown this *irx7*+ intermediate domain to

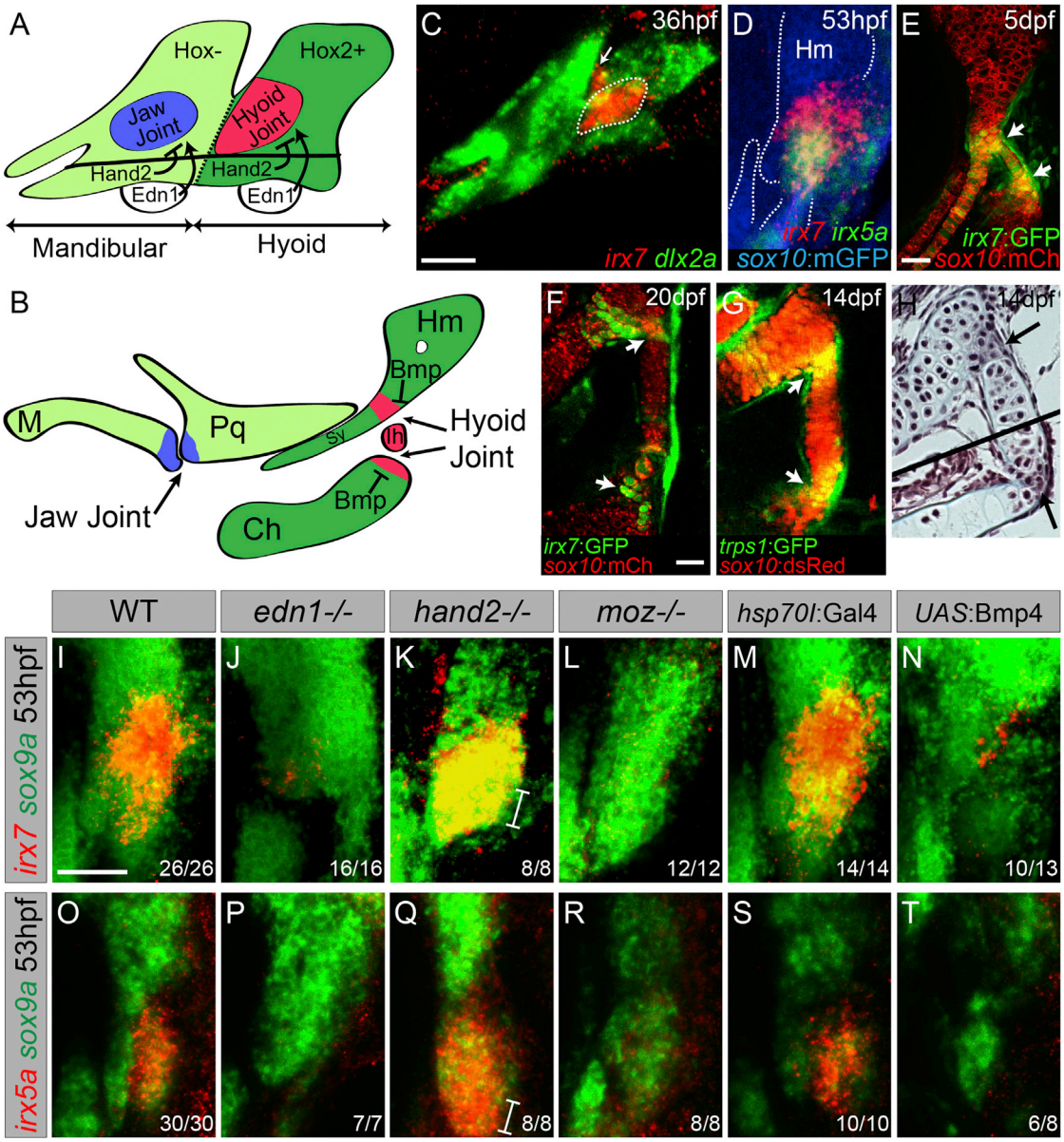

Figure 1. Regulation of *irx7* and *irx5a* Expression and Character of the Hyoid Joint

(A and B) Schematics of mandibular and hyoid arches at 36 hpf and cartilage derivatives at 5 dpf show early regulation of joints by Hand2 and Edn1 and late regulation by Bmp signaling.

(C) In situ hybridization at 36 hpf shows expression of *irx7* (red) relative to *dlx2a*+ neural-crest-derived cells (green) in a domain of intermediate hyoid arch cells (dashed line) and in a portion of the first pharyngeal pouch (arrow).

(D) Relative to *sox10*:GFPCAAX+ cartilages (anti-GFP, blue), overlapping expression of *irx7* (red) and *irx5a* (green) is seen at the developing hyoid joint.

(E and F) An *irx7*:GFP gene-trap line (green) shows increasingly restricted expression at the bipartite hyoid joint (arrows) relative to *sox10*:mCherryCAAX+ cartilages (red).

(G) *trps1*:GFP labels a similar population of cells as *irx7* at each side of the hyoid joint (arrows) relative to *sox10*:dsRed+ cartilages.

(H) Trichrome staining shows that cells at the hyoid joints (arrows) are smaller and lack the large lacunae of neighboring hypertrophic chondrocytes. Black line denotes merging of two adjacent sections.

(I–T) Expression of *irx7* and *irx5a* (red) relative to *sox9a*+ hyoid chondrocytes (green) in *edn1*, *hand2*, and *moz* mutants, as well as *hsp70l*:Gal4 control and *hsp70l*:Gal4; *UAS*:Bmp4 embryos subjected to 40–44 hpf heat shock. Brackets show ventral expansion in *hand2* mutants. M, Meckel's; Pq, palatoquadrate; Sy, symplectic; Hm, hyomandibula; Ch, ceratohyal; Ih, interhyal. Numbers indicate proportion of animals showing the displayed phenotype.

Scale bars represent 30 μM. See also Figure S1.

contribute to the hyoid joint and a joint-proximal extension of cartilage called the symplectic (Crump et al., 2006). At the onset of chondrogenesis (53 hpf), multicolor fluorescent in situs revealed overlapping expression of *irx7* and *irx5a* at the developing hyoid joint, as well as in a zone connecting the nascent hyomandibular and symplectic cartilages (Figure 1D). By 72 hpf, *irx7* and

irx5a became further restricted to cells within and surrounding the hyoid joint, with additional *irx5a* expression along the posterior margin of the hyoid arch (Figure S1). Analysis of a SAGp11A gene-trap line, in which GFP was inserted in the *irx7* locus (Kawakami et al., 2004), confirmed *irx7* expression in the developing hyoid joint, as well as continued expression in the joint until at least 20-days post-fertilization (dpf) (Figures 1E, 1F, and S1). A comparison of *irx7*:GFP and *trps1*:GFP lines further shows that *irx7*-expressing cells maintain the immature chondrocyte marker *trps1* (Figures 1F and 1G). Histology reveals that *irx7* expression corresponds to two zones of compact chondrocytes that connect either side of the interhyal cartilage with hyomandibular and ceratohyal cartilages, which are themselves composed of larger chondrocytes embedded in lacunae (Figure 1H). Live imaging of *sox10*:dsRed+ chondrocytes shows that the larval hyoid joint functions as a hinge during respiration (Movie S1). Although the hyoid joint shows no cavitation, this motility and lack of chondrocyte hypertrophy at the joint are reminiscent to that seen at mammalian hinge joints, such as the interphalangeal joints of the digits.

In the mandibular arch, *nkx3.2* (*bapx1*), which is required for jaw joint formation, is restricted to the intermediate domain by positive Edn1 and negative Hand2 function (Miller et al., 2003). Likewise, we find *irx7* and *irx5a* expression to be lost in *edn1* mutants and ventrally expanded in *hand2* mutants (Figures 1I–1K and 1O–1Q). Whereas the jaw joint gene *nkx3.2* is excluded from the hyoid arch by Moz-dependent Hox2 expression (Miller et al., 2004), hyoid joint expression of *irx7* and *irx5a* instead requires Moz (Figures 1L and 1R). Similar dorsoventral signaling pathways therefore restrict *irx7/5a* and *nkx3.2* to the joint-forming regions of the hyoid and mandibular arches, respectively, with Hox2 genes promoting the expression of *irx7* at the expense of *nkx3.2* in the hyoid arch.

In previous work, we had shown that Bmp signaling has a distinct role from Edn1 in specifying ventral at the expense of intermediate/joint fates (Zuniga et al., 2011). Here, by using a heat-shock-inducible Gal4/UAS system, we find that misexpression of Bmp4 ligand during later chondrogenic stages (40–44 hpf) disrupts hyoid joint formation without affecting overt dorsoventral patterning (Figure S1). These joint defects correspond with a loss of *irx7* and *irx5a* expression in the hyoid arch, indicating that Bmp signaling negatively regulates Irx gene expression (Figures 1N and 1T). Moreover, this loss of Irx expression is not solely due to the reported upregulation of Hand2 by Bmp4 (Zuniga et al., 2011), as either early (20–24 hpf) or late (40–44 hpf) Bmp4 misexpression still inhibits *irx7* expression in embryos lacking *hand2* (Figure S1). Thus, distinct from its early role in dorsoventral patterning, Bmp signaling has a later role in restricting *irx7/5a* expression to the developing hyoid joint.

Irx7 and Irx5a Are Necessary for Hyoid Joint Formation

In order to assess requirements in hyoid joint development, we used TALE nucleases to generate early frame-shift alleles for *irx7* and *irx5a* (Figures 2A and 2B). Whereas single *irx5a*^{el574} mutants had no apparent defects, 63% of *irx7*^{el538} mutants and 100% of *irx7*^{el538}; *irx5a*^{el574} double mutants displayed specific losses of the hyoid joint. In the WT hyoid joint, cells on either side of the interhyal cartilage stain poorly with Alcian, a dye that detects sulfated proteoglycans characteristic of cartilage matrix (Figure 2C). In contrast, *irx7*^{el538} and *irx7*^{el538}; *irx5a*^{el574} mutants had increased Alcian staining across the presumptive hyoid joint, with cells within the mutant hyoid interzone appearing larger than their WT counterparts (Figures 2D and 2E). Defects were also exclusive to the hyoid joint, consistent with the highly localized expression of *irx7*. Some *irx7*^{el538}; *irx5a*^{el574} double mutants were adult viable despite the persistence of the fused hyoid joint (Figure 2G), with no apparent defects in other joints (including the jaw joint). In order to confirm that the observed phenotypes were due to loss of *irx7* and *irx5a*, we also generated independent *irx7*^{el540} and *irx5a*^{e576} alleles and observed the same specific hyoid joint defects, either in *irx7*^{el540} alone or in all combinations of *irx7* and *irx5a* alleles (Figure S2). We did not, however, observe the body axis defects reported using *irx7* morpholinos, although we cannot exclude residual Irx7 protein in our mutants (Zhang et al., 2012). We also found no evidence in mutants for cross-regulation of *irx7* and *irx5a* expression (Figure S2).

A related phenotype resulting from loss of *irx7* was a shorter symplectic, which forms by the radial intercalation of cells adjacent to the nascent hyoid joint. In both *irx7*^{el538} and *irx7*^{el538}; *irx5a*^{el574} mutants, the symplectic was composed of 30% fewer chondrocytes than in WT siblings (Figure S2). This loss of symplectic cells was reflected in a corresponding cell increase in the zone connecting the hyomandibula and symplectic, with total chondrocyte numbers unaffected. As previous time-lapse imaging had shown that symplectic cells originate from this connecting zone (Crump et al., 2004), Irx7/5a may thus be required for chondrocytes to rearrange into an extending symplectic. Interestingly, *nkx3.2*-deficient embryos also lack an element (the retroarticular) adjacent to the jaw joint (Miller et al., 2004), indicating common requirements for Irx7/5a and Nkx3.2 in coordinating joint formation with associated perichondral bones.

Irx7 Inhibits Cartilage Differentiation Cell Autonomously

In order to examine whether Irx7 functions within developing chondrocytes to inhibit their maturation, we performed early gastrula-stage transplants of *hsp70l*:Gal4; *UAS*:Irx7-T2A-GFP neural crest precursors, or control *hsp70l*:Gal4; *UAS*:kikGR precursors, into WT *sox10*:dsRed hosts. This *sox10*:dsRed transgene shows two waves of expression: first in all arch neural-crest-derived cells and then in chondrocytes. Subsequent heat shocks from 30–34 hpf induced clones of donor cells expressing Irx7/GFP or the control kikGR fluorescent protein within arches otherwise populated by *sox10*:dsRed+ host cells (Figure 2H). Whereas both kikGR- and Irx7/GFP-expressing donor cells efficiently populated the pharyngeal arches of hosts at 48 hpf, Irx7/GFP-expressing cells contributed to cartilage in only 15% of hosts at 4 dpf compared with 90% of hosts for control cells (Figures 2I–2O). The inefficient incorporation of Irx7/GFP-expressing cells into cartilage was not simply due to their loss as they extensively contributed to hyoid bones and ligaments. Moreover, in the 15% of hosts in which Irx7/GFP-expressing cells incorporated into cartilages, we observed decreased Alcian staining in a largely cell-autonomous manner (Figures 2Q and 2S). Irx7 thus acts very locally to block Alcian+ matrix production. At the normal hyoid joint, this paucity of Alcian+ cartilage matrix might contribute to the flexibility of attachment points.

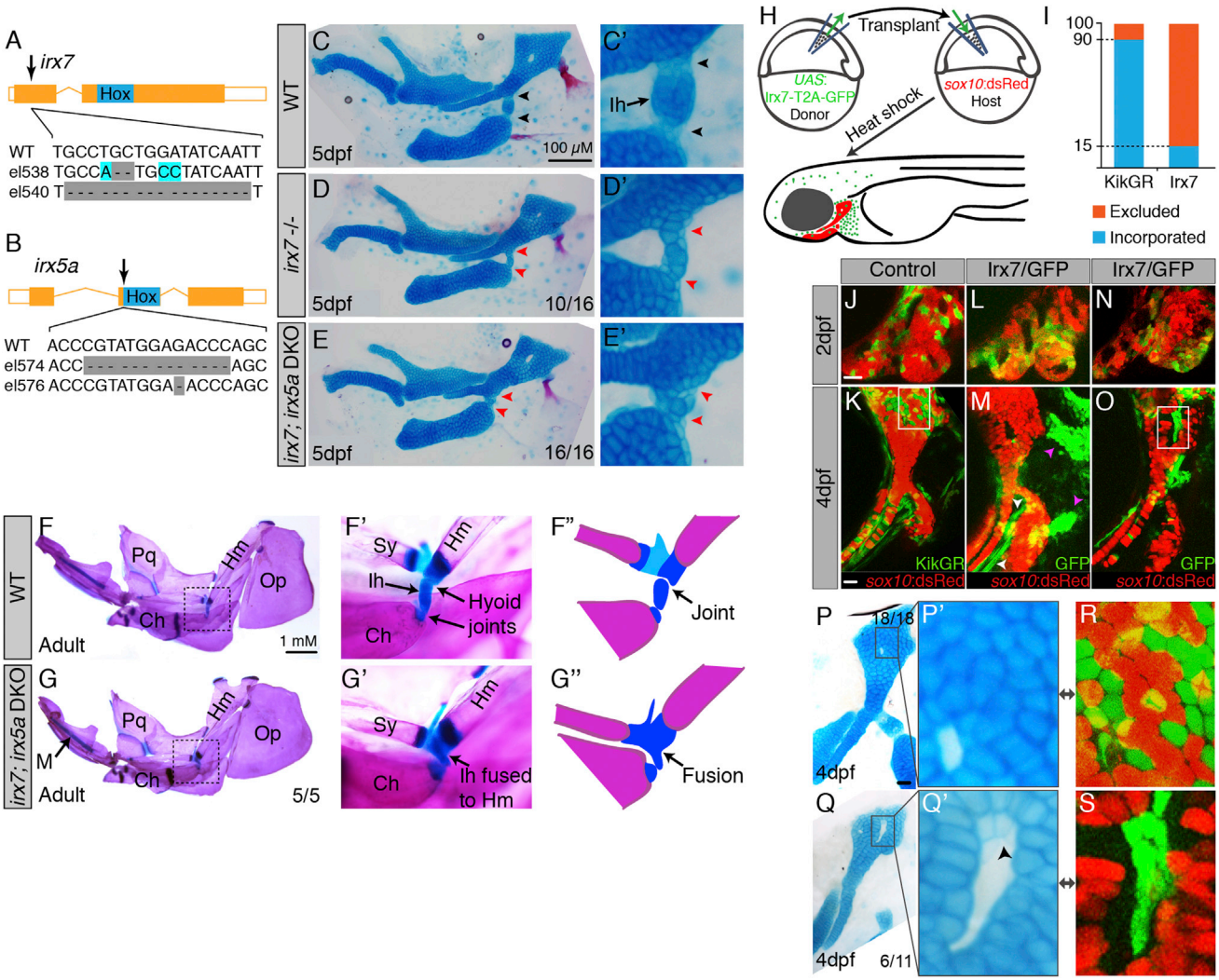

Figure 2. Requirements of Irx7 and Irx5a in Hyoid Joint Formation

(A and B) Schematics of *irx7* and *irx5a* TALEN mutants show the position of out-of-frame deletions (arrows) relative to homeobox domains (blue boxes).

(C–E) Lateral views of mandibular and hyoid skeletons (left) and magnified views of the hyoid joints (right) show cartilages (Alcian Blue) and bones (Alizarin Red) at 5 dpf. In WT, hyoid joint cells on either side of the Ih cartilage stain poorly with Alcian (black arrowheads). In $irx7^{el538}$ and $irx7^{el538}$; $irx5a^{el574}$ mutants, the hyoid joint is dysmorphic with increased Alcian reactivity (red arrowheads).

(F and G) Dissected adult zebrafish facial skeletons (3-months post-fertilization; size matched). The hyoid joint (dashed box) is magnified in (F') and (G') and schematized in (F") and (G") to show joint fusions in $irx7^{el538}$; $irx5a^{el574}$ double mutants. Op, opercular bone.

(H) Scheme of neural crest transplants followed by 30–34 hpf heat shocks to induce donor transgene expression.

(I) Whereas control kikGR-expressing cells contributed to hyoid cartilage in 18 of 20 cases, Irx7/GFP-expressing cells contributed to cartilage in only 11 of 72 cases (Fisher's exact two-tailed test, $p < 0.0001$).

(J–O) *sox10*:dsRed hosts received either control *hsp70l*:Gal4; *UAS*:kikGR or *hsp70l*:Gal4; *UAS*:Irx7-T2A-GFP donor neural crest precursors. Imaging at 2 dpf revealed contribution of donor cells to the mandibular and hyoid arches, and re-imaging at 4 dpf revealed contributions to *sox10*:dsRed+ hyoid cartilage. Arrowheads indicate contribution of Irx7/GFP-expressing cells to ligaments (white) and bones (magenta).

(P–S) Cell-specific loss of Alcian reactivity is seen in donor cells expressing Irx7/GFP (magnified in Q'; S is boxed region from O) but not kikGR (magnified in P'; R is boxed region from K). Numbers indicate proportion of animals showing the displayed phenotype.

Scale bars represent 20 μM unless otherwise noted. See also Figure S2.

Irx7 Arrests Chondrocyte Maturation at the Hyoid Joint

We next examined the mechanism by which Irx7 inhibits the deposition of Alcian+ matrix at the hyoid joint. As in mammals, zebrafish chondrocytes initially express SoxE factors (*sox9a* and *sox10*) and the *trps1* gene (Nichols et al., 2013). Maturing chondrocytes then downregulate *trps1* and upregulate a number of genes, in particular major constituents of cartilage matrix such as type II collagen (*col2a1a*) and aggrecan (*acana*). In $irx7^{el538}$ mutants, we observed that *trps1*:GFP expression was reduced in the larval hyoid joint (Figures 3A and 3B). We also observed elevated *col2a1a* and *acana* expression and Col2a1 protein across the hyoid joint of $irx7^{el538}$ mutants (Figures 3C–3H). Further, we found that zebrafish Irx7 was sufficient to inhibit Alcian+ cartilage matrix production and *Col2a1* and *Acan*

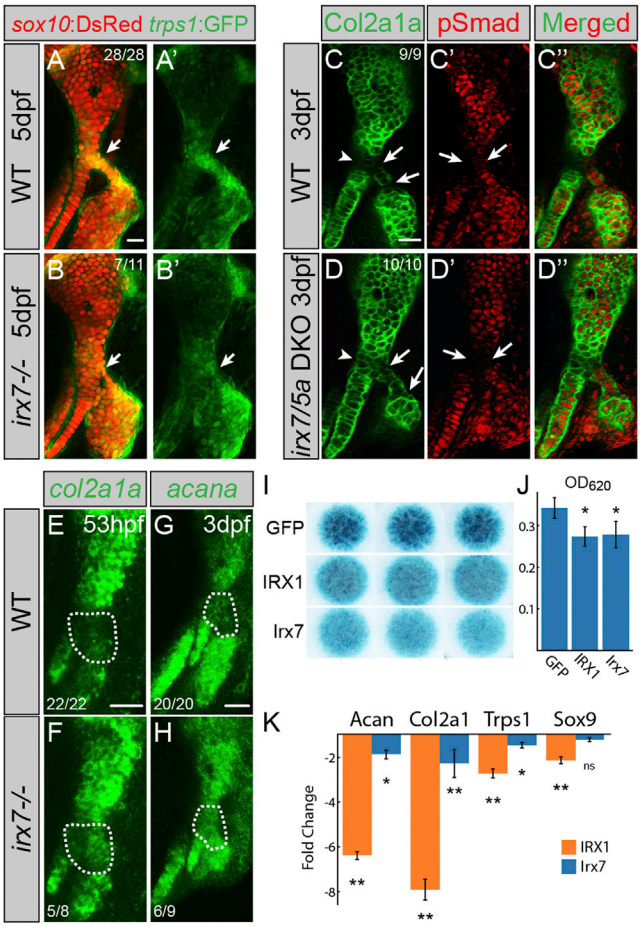

Figure 3. Irx7 Represses Chondrocyte Maturation

(A and B) *trps1*:GFP (green) is reduced at the hyoid joint (arrows) of *irx7*^{el538} mutants compared with WT siblings. *sox10*:dsRed labels hyoid cartilages (red).

(C and D) Immunostaining shows increased Col2a1a protein (green) but no change in phospho-Smad1/5/8 (red) in the hyoid joints (arrows) and Hm-Sy connecting zone (arrowheads) of *irx7*^{el538}; *irx5a*^{el574} mutants relative to WT siblings.

(E–H) In situ hybridization shows increased expression of *col2a1a* and *acana* in the hyoid joint region (dashed areas) of *irx7*^{el538} mutants relative to WT siblings. Numbers indicate proportion of animals showing the displayed phenotype. Scale bars represent 20 μM.

(I) Irx7 and murine IRX1 (but not GFP control) inhibit Alcian+ matrix accumulation in micromass cultures of ATDC5 cells grown in chondrogenic media for 7 days. Results were consistent across biological triplicates.

(J) Alcian blue content of the micromasses quantified by absorbance at 620 nm.

(K) qRT-PCR on RNA extracted from micromass cultures of ATDC5 cells grown in chondrogenic media for 7 days. Compared with GFP-expressing controls, expression of *Col2a1*, *Acan*, *and Trps1* was reduced by IRX1 and Irx7 misexpression. *Sox9* expression was reduced by IRX1 but not Irx7 misexpression. Error bars represent 95% confidence interval of the mean. *p < 0.05 and **p < 0.01 using Tukey HSD test.

See also Figure S3.

expression in chondrogenic murine ATDC5 cells cultured as micromasses. Intriguingly, mouse IRX1 could similarly inhibit cartilage matrix production and gene expression, suggesting that inhibition of chondrocyte maturation may be a more general property of vertebrate Irx proteins (Figures 3I–3K). Compared with inhibition of *Col2a1* and *Acan* expression, *Sox9* expression was unaffected by Irx7 misexpression and only modestly decreased by IRX1, consistent with Irx proteins functioning largely downstream of Sox9 to inhibit type II collagen and Aggrecan production. Irx7/IRX1 misexpression also modestly decreased *Trps1* expression. That Irx7 is required for *trps1*:GFP expression at the zebrafish hyoid joint but not sufficient to induce *Trps1* in vitro might reflect an indirect role of Irx7 in regulating *Trps1*, in line with previous data that Irx proteins function largely as transcriptional repressors (Cavodeassi et al., 2001).

We also find that Irx7 regulates cartilage maturation independently of Bmp signaling. Both WTs and *irx7*^{el538}; *irx5a*^{el574} mutants had similarly lower levels of Bmp activity at the hyoid joint compared with neighboring chondrocytes, as assessed by phosphorylation of Smad1/5/8 (Figures 3C' and 3D'). Combined with the ability of Bmp4 to inhibit *irx7* and *irx5a* expression, these findings imply that Irx7/5a function downstream of Bmp signaling to inhibit chondrocyte maturation at the hyoid joint. Interestingly, we found the zone connecting the symplectic and hyomandibula also to be low in *col2a1a* and *acana* in WTs, with increased *col2a1a* and *acana* in *irx7*^{el538} mutants. The inability to maintain chondrocytes in an immature state may thus explain not only hyoid joint fusions but also the shortening of the joint-proximal symplectic cartilage in mutants, with accelerated cartilage matrix production entrapping cells before they can rearrange into stacks.

Irx7 Directly Inhibits a *col2a1a* Enhancer

While our cell culture studies indicate that Irx proteins are sufficient to inhibit *Col2a1* and *Acan* expression, this could reflect Irx binding to either protein co-factors or DNA regulatory regions. We therefore investigated whether Irx7 might inhibit *col2a1a* expression in zebrafish through binding to a well-characterized cartilage-specific "R2" enhancer (Dale and Topczewski, 2011). As with endogenous Col2a1a mRNA and protein and a newly constructed *col2a1a* BAC transgene, we find that an *R2*:GFP transgene is low at the WT hyoid joint and upregulated in *irx7*^{el538} mutant joints (Figure 4A). Based on previous analysis of human (Jolma et al., 2013; Wingender et al., 2013) and *Drosophila* (Bilioni et al., 2005) consensus Iroquois binding motifs (ACA-nn/nnn-ACA and ACA-nn/nnn-TGT), we identified four putative Irx sites in the R2 enhancer. Whereas deletion of the second through fourth sites had no affect on *R2*:GFP expression, deletion of the first Irx site resulted in near complete loss of cartilage expression (Figure 4B). As this Irx site overlaps with a predicted Sox9 binding site (Mathelier et al., 2014), we reasoned that loss of Sox9 binding to this enhancer might account for the loss of cartilage transgene expression. Consistently, deleting only a portion of the Irx site without affecting the Sox9 site, or replacing it with a consensus Sox9-binding site lacking the Irx site, resulted in ectopic transgene expression within the hyoid joint (Figure 4B). An electrophoretic mobility shift assay further confirmed that both Sox9a and Irx5a proteins bind this overlapping site in vitro (Figure 4C). An attractive model then is that Irx proteins compete with or modify Sox9a activity at the R2 enhancer, thus dampening Sox9a-mediated activation of *col2a1a*. As Irx5 and Trps1 form a transcriptional complex with Irx3 in *Xenopus* (Bonnard et al., 2012), it will be interesting to test whether a similar complex involving Irx5a, Trps1, and Irx7 represses the

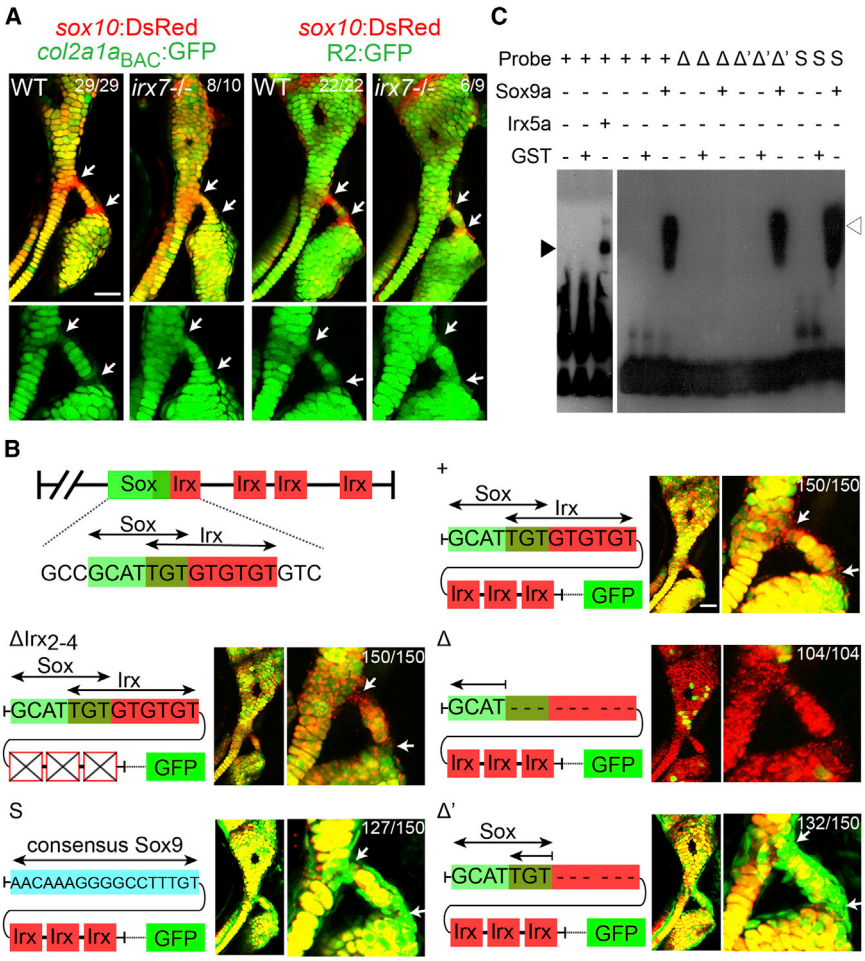

Figure 4. Irx Genes Directly Repress a *col2a1a* Enhancer

(A) Relative to *sox10*:dsRed+ chondrocytes (red), *col2a1a*$_{BAC}$:GFP, and *R2*:GFP transgenes (green) show increased *col2a1a*-driven expression in hyoid joint cells (arrows) of *irx7*^{el538} mutants compared with WT siblings.

(B) Schematics show predicted Sox and Irx binding sites within the R2 enhancer of the *col2a1a* gene, as well as modified transgenic constructs. Confocal images at 6 dpf show the connection of the hyosymplectic and ceratohyal cartilages, with magnified images showing the bipartite hyoid joints (arrows). In all panels, the WT *col2a1a*$_{BAC}$:mCherry-NTR transgene (red) displays lower levels in hyoid joints cells than neighboring chondrocytes. Transgenes with WT or modified R2 enhancers driving GFP are shown in green. Both the WT R2 enhancer and a version missing the second through fourth putative Irx sites are similar to WT *col2a1a*$_{BAC}$:mCherry-NTR in being excluded from joints (yellow reflects overlap). Loss of the overlapping Sox/Irx site of the R2 enhancer abolishes most cartilage expression (red), and replacement with a Sox9 consensus site or deletion of just the Irx half-site results in ectopic joint expression (green). In the case of R2 enhancer missing the overlapping Sox/Irx site (Δ) 104 animals injected with the plasmid show similar expression and out of 30 founders screened, none showed more than just a sparse GFP expression in a few cartilage cells. For other panels experimental numbers are pooled for three independent stable transgenic lines. 50 embryos were examined for each line. Numbers indicate the proportion of animals showing the displayed phenotype. Scale bars represent 30 μM.

(C) An electrophoretic mobility shift assay shows binding of Irx5a (closed arrowhead) and Sox9a (open arrowhead) but not a control GST protein to a probe containing the wild-type Sox/Irx site (+). Sox9a binds a probe deleted for the Irx half-site (Δ') but not the entire Sox/Irx site (Δ), and binding is restored by replacement of the Sox/Irx site with a consensus Sox9 binding site (S).

See also Figure S4.

expression of *col2a1a*, *acana*, and other chondrocyte matrix genes at the hyoid joint.

Remarkably, the existence of a hyoid joint only in fishes precisely correlates with presence of the *irx7* gene in all sequenced fish genomes (including coelacanths) but not in any known tetrapod genome. During the transition to land, the hyoid skeleton that originally connected the jaw to the ear evolved to acquire a new function in sound transduction, with the columella and then stapes (both viewed as hyomandibula homologs) retreating into the middle ear and losing their connections to the hyoid bone (homologous to the fish ceratohyal). One possibility then is that loss of the hyoid joint during ear evolution resulted in the *irx7* gene becoming dispensable for development, hence resulting in its loss from tetrapod genomes (see Figure S3 for a potential evolutionary history of *irx7*).

While the unique requirement of a single Irx gene at the zebrafish hyoid joint has allowed us to uncover roles for Irx7 in repressing chondrocyte maturation, this function likely extends to other members of the Irx family. First, loss of *irx5a*, a homolog of one of the members of the mammalian *Irx3/5/6* cluster, enhances joint defects in *irx7* mutants. Second, deletion of the Irx binding site from the *col2a1a* enhancer also results in ectopic expression at the mandibular and hyomandibula-otic joints (Figures S4A–S4C). Third, we observe expression of *irx1b* at the joint connecting the pectoral fin to the girdle, which corresponds to a zone of high Sox10 and low Col2a1 and Alcian+ matrix as seen in the hyoid joint (Figures S4D–S4F). Fourth, we find that *Irx1* and *Col2a1* expression similarly anti-correlates in the developing interphalangeal joints of the mouse paw (Figures S4G–S4I). Fifth, both zebrafish Irx7 and murine IRX1 are able to inhibit cartilage matrix production in a chondrogenic cell line. In the future, it will be interesting to examine the extent to which diverse members of the Irx family function to restrain the Sox9-mediated maturation of chondrocytes, including not only at joints but also within the periochondrium and other locations where cartilage differentiation needs to be tightly controlled.

EXPERIMENTAL PROCEDURES

Zebrafish Lines

Zebrafish (*Danio rerio*) were staged as described (Kimmel et al., 1995). All procedures were approved by the University of Southern California Institutional

Animal Care and Use Committee. Reported lines include *edn1*^{tf216b} (Miller et al., 2000), *Df(chr01:hand2)s6* (Yelon et al., 2000), *moz*^{b719} (Miller et al., 2004), *trps1*^{l127aGt} (Talbot et al., 2010), *Tg(hsp70l:Gal4)*^{kca4} (Scheer and Campos-Ortega, 1999), *Tg(UAS:Bmp4; cmlc2:GFP)*^{el49} (Zuniga et al., 2011), *Tg(UAS:kikGR; α-crystallin:Cerulean)*^{el377}, and *Tg(sox10:dsRED)*^{el10} (Das and Crump, 2012). SAGp11A (*irx7:GFP*) was obtained from National Institute of Genetics (Kawakami et al., 2004; Nagayoshi et al., 2008).

Tg(UAS:Irx7-T2A-GFP; α-crystallin:Cerulean)^{el613}, Tg(sox10:GFPCAAX)^{el375}, and Tg(sox10:mCherryCAAX)^{el361} were generated by a one-cell-embryo injection of plasmids constructed with the Tol2kit (Kwan et al., 2007), and col2a1a$_{BAC}$:GFP and col2a1a$_{BAC}$:mCherry-NTR lines were generated according to Shin et al. (2003) (see Supplemental Experimental Procedures). Modified versions of the R2 enhancer were made using Integrated DNA Technologies GBlocks and cloned into the R2-E1b:EGFP plasmid (Dale and Topczewski, 2011). See Supplemental Experimental Procedures for sequences of modified R2 enhancers and probes for EMSA. Null alleles for *irx7* and *irx5a* were generated using the TALEN protocol of Sanjana et al. (2012). See Supplemental Experimental Procedures for details on the design of TALENs and genotyping assays. For heat-shock induction, embryos were placed in a 40°C incubator for 4 hr and then transferred to 28.5°C. All phenotypes were scored before genotyping.

Histology and Skeletal Analysis

Cartilage and bone staining and fluorescent in situ hybridizations (including *dlx2a* and *sox9a*) were performed as described (Zuniga et al., 2010). For all other genes, templates were amplified and cloned into pCR-Blunt II-TOPO vector for probe synthesis (see Supplemental Experimental Procedures, in situ probe templates). Immunohistochemistry was performed as described (Crump et al., 2004; Nichols et al., 2013) using mouse anti-Col2a1 (1:100; II-II6B3-DSHB) and anti-pSmad1/5/8 (1:200; gift of Ed Laufer) and secondary antibodies AlexaFluor488 goat anti-mouse (1:300; Life Technologies, A-11001) and AlexaFluor568 goat anti-rabbit (1:300; Life Technologies, A-11011). Staining with Trichrome/Gomori One-Step/Aniline Blue Kit was performed per manufacturer instructions (Newcomersupply).

Transplants

As described in Crump et al. (2004), donor cells from *UAS:kikGR*; *hsp70l:Gal4* or *UAS:Irx7-T2A-GFP*; *hsp70l:Gal4* embryos were transplanted into the neural crest precursor domain of *sox10:dsRed* embryos at 6 hpf. Embryos were subjected to heat shock from 30–34 hpf to activate transgene expression, imaged by a confocal microscope at 48 hpf and 4 dpf and fixed at 4 dpf for skeletal staining.

Imaging

Confocal microscopy was performed on a Zeiss LSM5 microscope using ZEN software. Skeletons were imaged on a Leica DM2500 microscope. Levels were adjusted in Adobe Photoshop CS5, with identical adjustments applied to images from the same dataset.

In Vitro Cartilage Differentiation Assay

Retroviral expression vectors, pMXs_GFP-P2A-IRX1, pMXs_Irx7-T2A-GFP, and pMXs_GFP, were assembled by Gateway cloning (Invitrogen), and transduction was performed as described Takahashi et al. (2007). ATDC5 cells were infected with two pools of viral supernatant during a 48-hr period. GFP-positive cells were FACS purified and cultured as micromasses at a density of 10^5 cells per well. Samples were collected at day 7 of culture. Continued transgene expression was confirmed by qRT-PCR for GFP, *irx7*, *Irx1*, and *Gapdh* (see Supplemental Experimental Procedures). In vitro cartilage induction and qRT-PCR was performed as described (Brown et al., 2008; Schmittgen and Livak, 2008). qPCR data were analyzed using $\Delta\Delta C_T$ method. See Supplemental Experimental Procedures for extended details and sequence of qPCR primers.

Electrophoretic Mobility Shift Assay

Zebrafish Irx5a and Sox9a and negative control GST proteins were translated using the PURExpress in vitro protein synthesis kit (NEB). Biotin-labeled probes were obtained from IDT (see Supplemental Experimental Procedures, sequences of modified R2 enhancers and probes for electrophoretic mobility shift assay [EMSA]). Proteins and probes in binding buffer were incubated at room temperature for 30 min and then run on a 5% TBE polyacrylamide gel. Chemiluminescent nucleic acid detection was performed per manufacturer instructions (Pierce).

Statistical Analysis

Fisher's exact two-tailed test was used to test the significance of Irx7 overexpression on contribution of donor cells to cartilage (Figure 2I). The percentage of transplanted animals in which donor cells contributed to the cartilage is shown in each case. One-way ANOVA followed by Tukey-Kramer HSD test was performed for multiple pairwise comparisons (Figures 3J, 3K, and S2H). Error bars show 95% confidence interval of the mean.

SUPPLEMENTAL INFORMATION

Supplemental Information includes Supplemental Experimental Procedures, four figures, and one movie and can be found with this article online at http://dx.doi.org/10.1016/j.devcel.2015.10.004.

AUTHOR CONTRIBUTIONS

A.A., L.M., S.P, S.D., and R.D. performed the experiments. X.H., A.K.I., S.G., J.K.I., A.P.M, and F.V.M. assisted with mammalian experiments. A.A. and J.G.C. wrote the manuscript.

ACKNOWLEDGMENTS

We thank Megan Matsutani and Jennifer DeKoeyer Crump for fish care, Ed Laufer for the pSmad1/5/8 antibody, and Koichi Kawakami and the National BioResource Project for the SAGp11A line. Funding was by NIH R01 DE018405 and March of Dimes (J.G.C.), NIH T32 (A.A. and L.M.) and Giannini (L.M.) fellowships, and the Loyola University Chicago's Provost office (R.M.D. and S.D.).

Received: December 19, 2014
Revised: September 28, 2015
Accepted: October 7, 2015
Published: November 9, 2015

REFERENCES

Archer, C.W., Dowthwaite, G.P., and Francis-West, P. (2003). Development of synovial joints. Birth Defects Res. C Embryo Today *69*, 144–155.

Bilioni, A., Craig, G., Hill, C., and McNeill, H. (2005). Iroquois transcription factors recognize a unique motif to mediate transcriptional repression in vivo. Proc. Natl. Acad. Sci. USA *102*, 14671–14676.

Bonnard, C., Strobl, A.C., Shboul, M., Lee, H., Merriman, B., Nelson, S.F., Ababneh, O.H., Uz, E., Güran, T., Kayserili, H., et al. (2012). Mutations in IRX5 impair craniofacial development and germ cell migration via SDF1. Nat. Genet. *44*, 709–713.

Brown, A.J., Alicknavitch, M., D'Souza, S.S., Daikoku, T., Kirn-Safran, C.B., Marchetti, D., Carson, D.D., and Farach-Carson, M.C. (2008). Heparanase expression and activity influences chondrogenic and osteogenic processes during endochondral bone formation. Bone *43*, 689–699.

Brunet, L.J., McMahon, J.A., McMahon, A.P., and Harland, R.M. (1998). Noggin, cartilage morphogenesis, and joint formation in the mammalian skeleton. Science *280*, 1455–1457.

Cavodeassi, F., Modolell, J., and Gómez-Skarmeta, J.L. (2001). The Iroquois family of genes: from body building to neural patterning. Development *128*, 2847–2855.

Craft, A.M., Ahmed, N., Rockel, J.S., Baht, G.S., Alman, B.A., Kandel, R.A., Grigoriadis, A.E., and Keller, G.M. (2013). Specification of chondrocytes and cartilage tissues from embryonic stem cells. Development *140*, 2597–2610.

Crump, J.G., Swartz, M.E., and Kimmel, C.B. (2004). An integrin-dependent role of pouch endoderm in hyoid cartilage development. PLoS Biol. *2*, E244.

Crump, J.G., Swartz, M.E., Eberhart, J.K., and Kimmel, C.B. (2006). Moz-dependent Hox expression controls segment-specific fate maps of skeletal precursors in the face. Development *133*, 2661–2669.

Dale, R.M., and Topczewski, J. (2011). Identification of an evolutionarily conserved regulatory element of the zebrafish col2a1a gene. Dev. Biol. *357*, 518–531.

Das, A., and Crump, J.G. (2012). Bmps and id2a act upstream of Twist1 to restrict ectomesenchyme potential of the cranial neural crest. PLoS Genet. *8*, e1002710.

Francis-West, P.H., Parish, J., Lee, K., and Archer, C.W. (1999). BMP/GDF-signalling interactions during synovial joint development. Cell Tissue Res. *296*, 111–119.

Gomez-Skarmeta, J.L., Diez del Corral, R., de la Calle-Mustienes, E., Ferré-Marcó, D., and Modolell, J. (1996). Araucan and caupolican, two members of the novel iroquois complex, encode homeoproteins that control proneural and vein-forming genes. Cell *85*, 95–105.

Grotewold, L., and Rüther, U. (2002). The Fused toes (Ft) mouse mutation causes anteroposterior and dorsoventral polydactyly. Dev. Biol. *251*, 129–141.

Hartmann, C., and Tabin, C.J. (2001). Wnt-14 plays a pivotal role in inducing synovial joint formation in the developing appendicular skeleton. Cell *104*, 341–351.

Hootman, J.M., Helmick, C.G., and Brady, T.J. (2012). A public health approach to addressing arthritis in older adults: the most common cause of disability. Am. J. Public Health *102*, 426–433.

Jolma, A., Yan, J., Whitington, T., Toivonen, J., Nitta, K.R., Rastas, P., Morgunova, E., Enge, M., Taipale, M., Wei, G., et al. (2013). DNA-binding specificities of human transcription factors. Cell *152*, 327–339.

Kawakami, K., Takeda, H., Kawakami, N., Kobayashi, M., Matsuda, N., and Mishina, M. (2004). A transposon-mediated gene trap approach identifies developmentally regulated genes in zebrafish. Dev. Cell *7*, 133–144.

Kimmel, C.B., Ballard, W.W., Kimmel, S.R., Ullmann, B., and Schilling, T.F. (1995). Stages of embryonic development of the zebrafish. Dev. Dyn. *203*, 253–310.

Kwan, K.M., Fujimoto, E., Grabher, C., Mangum, B.D., Hardy, M.E., Campbell, D.S., Parant, J.M., Yost, H.J., Kanki, J.P., and Chien, C.B. (2007). The Tol2kit: a multisite gateway-based construction kit for Tol2 transposon transgenesis constructs. Dev. Dyn. *236*, 3088–3099.

Mathelier, A., Zhao, X., Zhang, A.W., Parcy, F., Worsley-Hunt, R., Arenillas, D.J., Buchman, S., Chen, C.Y., Chou, A., Ienasescu, H., et al. (2014). JASPAR 2014: an extensively expanded and updated open-access database of transcription factor binding profiles. Nucleic Acids Res. *42*, D142–D147.

McDonald, L.A., Gerrelli, D., Fok, Y., Hurst, L.D., and Tickle, C. (2010). Comparison of Iroquois gene expression in limbs/fins of vertebrate embryos. J. Anat. *216*, 683–691.

McNeill, H., Yang, C.H., Brodsky, M., Ungos, J., and Simon, M.A. (1997). mirror encodes a novel PBX-class homeoprotein that functions in the definition of the dorsal-ventral border in the Drosophila eye. Genes Dev. *11*, 1073–1082.

Miller, C.T., Schilling, T.F., Lee, K., Parker, J., and Kimmel, C.B. (2000). sucker encodes a zebrafish Endothelin-1 required for ventral pharyngeal arch development. Development *127*, 3815–3828.

Miller, C.T., Yelon, D., Stainier, D.Y., and Kimmel, C.B. (2003). Two endothelin 1 effectors, hand2 and bapx1, pattern ventral pharyngeal cartilage and the jaw joint. Development *130*, 1353–1365.

Miller, C.T., Maves, L., and Kimmel, C.B. (2004). moz regulates Hox expression and pharyngeal segmental identity in zebrafish. Development *131*, 2443–2461.

Nagayoshi, S., Hayashi, E., Abe, G., Osato, N., Asakawa, K., Urasaki, A., Horikawa, K., Ikeo, K., Takeda, H., and Kawakami, K. (2008). Insertional mutagenesis by the Tol2 transposon-mediated enhancer trap approach generated mutations in two developmental genes: tcf7 and synembryn-like. Development *135*, 159–169.

Nichols, J.T., Pan, L., Moens, C.B., and Kimmel, C.B. (2013). barx1 represses joints and promotes cartilage in the craniofacial skeleton. Development *140*, 2765–2775.

Peters, T., Ausmeier, K., Dildrop, R., and Ruther, U. (2002). The mouse Fused toes (Ft) mutation is the result of a 1.6-Mb deletion including the entire Iroquois B gene cluster. Mamm. Genome *13*, 186–188.

Sanjana, N.E., Cong, L., Zhou, Y., Cunniff, M.M., Feng, G., and Zhang, F. (2012). A transcription activator-like effector toolbox for genome engineering. Nat. Protoc. *7*, 171–192.

Scheer, N., and Campos-Ortega, J.A. (1999). Use of the Gal4-UAS technique for targeted gene expression in the zebrafish. Mech. Dev. *80*, 153–158.

Schmittgen, T.D., and Livak, K.J. (2008). Analyzing real-time PCR data by the comparative C(T) method. Nat. Protoc. *3*, 1101–1108.

Settle, S.H., Jr., Rountree, R.B., Sinha, A., Thacker, A., Higgins, K., and Kingsley, D.M. (2003). Multiple joint and skeletal patterning defects caused by single and double mutations in the mouse Gdf6 and Gdf5 genes. Dev. Biol. *254*, 116–130.

Shin, J., Park, H.C., Topczewska, J.M., Mawdsley, D.J., and Appel, B. (2003). Neural cell fate analysis in zebrafish using olig2 BAC transgenics. Methods Cell Sci. *25*, 7–14.

Takahashi, K., Okita, K., Nakagawa, M., and Yamanaka, S. (2007). Induction of pluripotent stem cells from fibroblast cultures. Nat. Protoc. *2*, 3081–3089.

Talbot, J.C., Johnson, S.L., and Kimmel, C.B. (2010). hand2 and Dlx genes specify dorsal, intermediate and ventral domains within zebrafish pharyngeal arches. Development *137*, 2507–2517.

Wingender, E., Schoeps, T., and Dönitz, J. (2013). TFClass: an expandable hierarchical classification of human transcription factors. Nucleic Acids Res. *41*, D165–D170.

Yelon, D., Ticho, B., Halpern, M.E., Ruvinsky, I., Ho, R.K., Silver, L.M., and Stainier, D.Y. (2000). The bHLH transcription factor hand2 plays parallel roles in zebrafish heart and pectoral fin development. Development *127*, 2573–2582.

Zhang, Y., Yang, Y., Trujillo, C., Zhong, W., and Leung, Y.F. (2012). The expression of irx7 in the inner nuclear layer of zebrafish retina is essential for a proper retinal development and lamination. PLoS ONE *7*, e36145.

Zuniga, E., Stellabotte, F., and Crump, J.G. (2010). Jagged-Notch signaling ensures dorsal skeletal identity in the vertebrate face. Development *137*, 1843–1852.

Zuniga, E., Rippen, M., Alexander, C., Schilling, T.F., and Crump, J.G. (2011). Gremlin 2 regulates distinct roles of BMP and Endothelin 1 signaling in dorsoventral patterning of the facial skeleton. Development *138*, 5147–5156.